Available online at www.sciencedirect.com

SciVerse ScienceDirect

Ceramics International 39 (2013) 3753–3758

CERAMICS INTERNATIONAL

www.elsevier.com/locate/ceramint

Characterization of a soldering system consisting of a glass from the system $CaO–Al_2O_3–B_2O_3–SiO_2$ and wollastonite

A. Schusser[a], M.J. Pascual[b,*], A. Prange[a], A. Durán[b], R. Conradt[a]

[a]*Institute of Mineral Engineering, Mauerstr. 5, 52064 Aachen, Germany*
[b]*Instituto de Cerámica y Vidrio (CSIC), Campus de Cantoblanco, 28049 Madrid, Spain*

Received 31 July 2012; received in revised form 15 October 2012; accepted 16 October 2012
Available online 24 October 2012

Abstract

In this work, the characterization of a soldering system with wollastonite as filler added as powder to the powdered base glass is shown. A soldering system consisting of the base glass and a coexisting crystalline phase is created which is then pressed to pellets and sintered to maximum density.

Wollastonite increases the thermal expansion coefficient of the base glass after sintering the samples. In the present paper, the sintering behavior of the soldering system and possible interactions between glass and filler are analyzed. Also, density and porosity after sintering and the resulting crystalline phases are characterized.

The mixtures with wollastonite contents up to 30% showed suitable sintering behavior and good density (low porosity). From 40% wollastonite on, the sintering of the samples was not satisfying and porosity was still high after sintering. The main crystalline phases were anorthite, wollastonite and pseudowollastonite, which occurred in all samples. This shows that all three phases are coexisting phases of the glass composition.

Keywords: A. Joining; B. Composites; C. Thermal expansion; D. Glass

1. Introduction

For use in aggressive media or at high temperatures, ceramic materials are always the number one choice due to their specific properties like their high melting point and chemical inertness. The bonding of ceramic parts can be performed by using soldering glasses or soldering systems consisting of a glassy and one or more crystalline phases [1,2]. The crystalline phases can either be added to the glass or be formed by crystallization of the glass itself.

The advantage of soldering systems is that they can be adapted to the needs of an industrial process without changing the chemically simple and easy to control base composition of the glass.

For a joining process in general, the coefficient of thermal expansion (CTE) is of particular interest [3]. The CTE of the solder has to match the CTE of the substrates that are joined. This is necessary to prevent the bonding from cracking because of thermally induced stresses.

Several authors already showed the possibility of increasing the CTE of a glass by adding different amounts of crystalline phases with a higher CTE [4,5,6]. The use of coexisting phases has been reported by Wanko [6]. In this work, a coexisting phase is used. The advantage of this is that a coexisting phase does not react with the glass and hence does not change the chemical composition and the properties of the base glass.

As shown in our previous work [7], it is possible to increase the CTE of a crystallized soldering glass by adding wollastonite as an aggregate before the crystallization. In this way, the properties of the soldering system can be custom-tailored to the demands of a certain industrial process. For example, the CTE of the base glass can be adapted to match with the CTE of the substrate to be joined.

In this work, the same base components (glass and wollastonite) like in the previous paper are used [7].

*Corresponding author.
E-mail addresses: mpascual@icv.csic.es (M.J. Pascual), conradt@ghi.rwth-aachen.de (R. Conradt).

0272-8842/$ - see front matter © 2012 Elsevier Ltd and Techna Group S.r.l. All rights reserved.
http://dx.doi.org/10.1016/j.ceramint.2012.10.213

The wollastonite amount and the processing parameter are optimized in order to get well sintered and homogeneous materials suitable for their application as a solder for ceramic components.

The characterization of the samples was done using hot stage microscopy, X-Ray diffraction and scanning electron microscopy. Additionally, the density of the samples before and after sintering was determined as well as the density of the powders which served as a threshold for the density of the samples at least before sintering. As the samples were at least partially crystalline after sintering, the density of the powder can only be a very rough estimate of the maximum density after sintering.

2. Experimental

The studied glass composition is 34.79 CaO, 18.09 Al_2O_3, 9.09 B_2O_3, 38.04 SiO_2 (wt%). The glass was prepared using chemical grade reagents: $CaCO_3$ (Merck, Germany), Al_2O_3 (Merck, Germany), H_3BO_3 (Merck, Germany) and amorphous SiO_2. The raw materials were mixed and heated to 1600 °C in a platinum crucible. After 3 h holding time, the glass melt was poured into cold water. The glass was characterized by differential thermal analysis (DTA) (Netzsch, Germany) using a heating rate of 15 K/min and dilatometer (Netzsch, Germany) employing a heating rate of 10 K/min. The glass was milled to powder with a size of < 63 μm employing an agata mortar.

The viscosity–temperature-curve of the pure glass was determined using the methods of rotational viscometry and hot stage microscopy (HSM). Additionally, the T_g was used where the viscosity was $\log\eta = 13.3$.

The viscosity of the glass was determined using the rotation method, employing a high-temperature Haake viscometer equipped with a ME 1700 sensor. The rotation procedure was applied for viscosity in the range 10^3–10^1 dPa s with a high temperature viscometer of the cylindrical Searle type at rotation speeds of 1–30 rpm for 10 min, following the International Standard ISO 7884-2. Three measurements were taken at three different rotation speeds for each temperature within this range. The use of both methods allows determination of the complete viscosity–temperature curve.

Hot Stage Microscopy (HSM) was performed in a Leica-EM201 microscope with image analysis for determination of the viscosity in air at a heating rate of 5 °C min^{-1}. The samples were initially cold pressed to conformed bodies of 3 mm in both height and diameter from glass powder. The temperature was measured with a Pt/Rh (6130) thermocouple placed under and in contact with the alumina support. The viscosities belonging to the characteristic temperatures of the glass were determined by HSM and were chosen according to [8].The wollastonite (Osthoff–Petrasch, Germany) was sintered at a temperature of 1200 °C. This was done because the structure of the wollastonite changed during the sintering from wollastonite to pseudowollastonite [4]. As a temperature of 1200 °C is easily reached during the sintering process, it was decided to pre-sinter the wollastonite and in this way simulate the soldering process. After sintering it was also milled to a size of < 63 μm.

Mixtures of the glass and wollastonite powders were prepared containing 0, 10, 20, 30, 40 and 50 wt% of wollastonite. Pellets were pressed from all the mixtures. The pellets had a diameter of 15 mm and a height of 3–7 mm. As the soldering process is a high-temperature process, the samples were sintered and crystallized during sintering.

The temperature programmes for sintering were chosen from HSM experiments. HSM experiments were performed on all mixtures and the pure glass. From the results, the temperatures corresponding to the maximum change of the area of the samples were determined for every sample (T_{sinter}). The derivatives of the area–temperature curves were calculated and the temperature at which the derivative showed the lowest value was chosen as T_{sinter}.

Each of the pellets was heated to T_{sinter} with a heating rate of 10 K/min and the temperature was held for 5 h to allow almost complete crystallization. After that, the furnace was turned off and the samples were left in the furnace to slowly cool down to room temperature.

X-ray diffraction (XRD) analysis (Bruker, Germany/USA) was used to determine the crystalline phases after sintering. The patterns were collected with monochromatic CuKα radiation over the range $5 \leq 2\theta \leq 90°$ with a step size of 3° and a fixed counting time of 96 s $step^{-1}$.

To ensure the gas tightness of the solder and make sure that the claimed properties are still maintained after addition of wollastonite, it is necessary to characterize the resulting soldering system according to porosity and density which was done by scanning electron microscopy (SEM) (Leo Electron Microscopy, United Kingdom). Additionally, the density of the sintered samples was determined using the principle of Archimedes in water. As the unsintered samples were not firm enough, their density could only be estimated by measuring their volume and weight in air. The densities of the original powders were measured using a gas pycnometer (Micromeritics, Germany).

3. Results and discussion

The T_g of the glass determined by DTA was 704 °C and the crystallization temperature was 972 °C. The DTA results were published in [7] and can be seen in Fig. 1. The CTE was found as $9.11 \times 10^{-6}\,K^{-1}$ (50–680 °C) and the CTE of the presintered wollastonite was measured as $13.41 \times 10^{-6}\,K^{-1}$ (200–800 °C).

The viscosity–temperature curve of the pure glass can be seen in Fig. 2. The characteristic temperatures are additionally shown in Table 1. Due to the crystallization of the glass during the experiments, not all the characteristic points could be measured. These were half sphere point

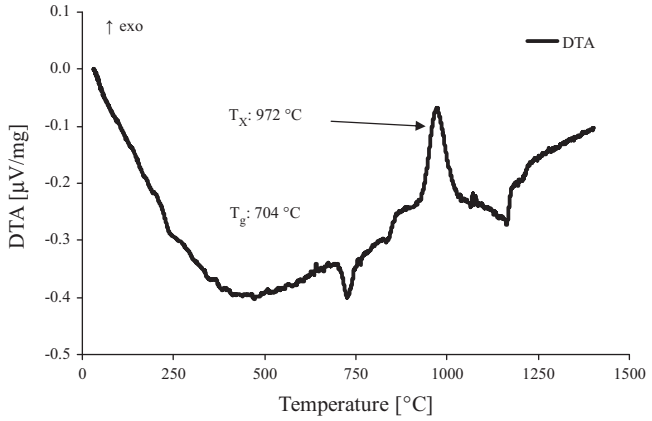

Fig. 1. DTA results for the pure glass [7].

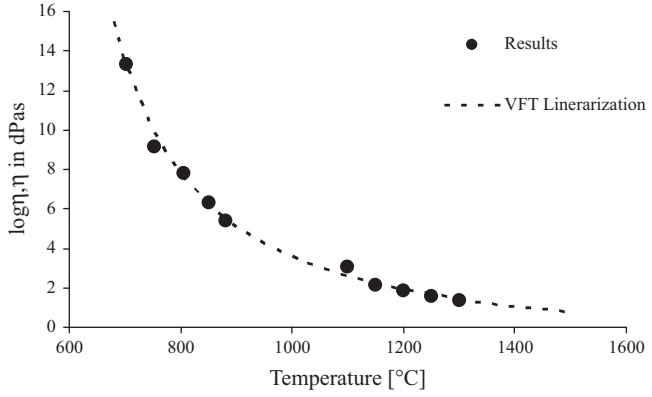

Fig. 2. Viscosity–temperature relation of the base glass.

Table 1
Characteristic temperatures of the pure glass.

Temperature [°C]	logη, η in dPas	Method of measurement
1300	1.34	Rotational viscometer
1250	1.57	
1200	1.83	
1150	2.14	
1100	3.02	
882	5.4	Hot stage microscopy
852	6.3	
807	7.8	
753	9.1	
704	13.3	DTA

and flow point from the HSM results. The VFT parameters were calculated by fitting of the VFT equation. They are displayed in Table 2.

The area–temperature curves as obtained by HSM can be found in Fig. 3, the calculated derivative for the sample containing 10 wt% of wollastonite is displayed in Fig. 4 as an example. The determined temperatures T_{sinter} can be found in Table 3 as well as the corresponding viscosity values obtained from the VFT equation. As can be seen, they increase with increasing amount of wollastonite up to

Table 2
VFT parameters of the pure glass.

A	−1.9
B	2564.1
T_0	533.0
Error	±0.32
Linearization parameter c	0.825

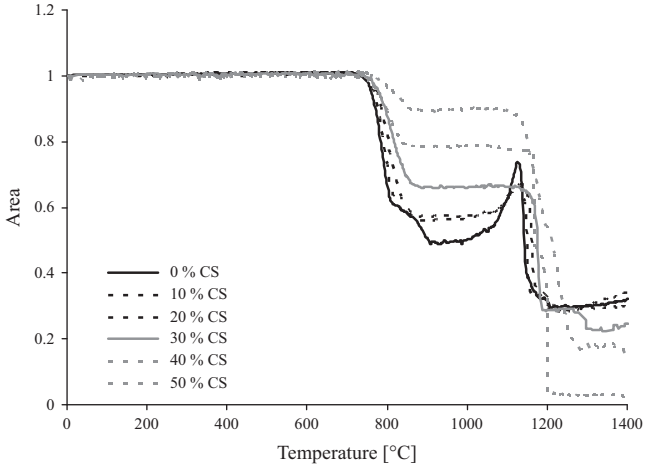

Fig. 3. Area–temperature curves for all samples determined by HSM.

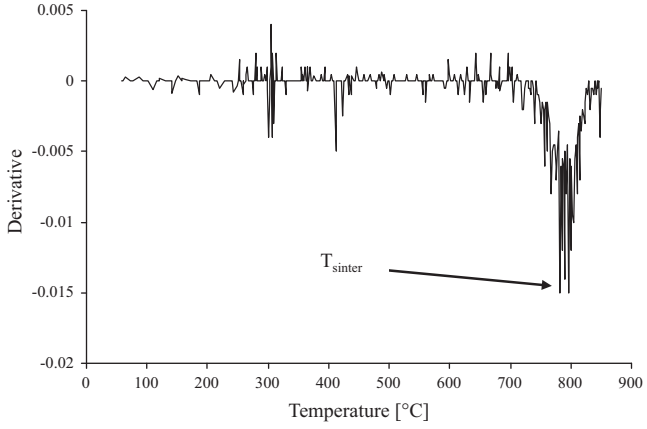

Fig. 4. Derivative of the area–temperature curve for the sample containing 10 wt% of wollastonite.

Table 3
Sintering temperatures (T_{sinter}) determined by HSM.

Sample	T_{sinter} [°C]
0% wollastonite	779
10% wollastonite	782
20% wollastonite	806
30% wollastonite	844
40% wollastonite	807
50% wollastonite	643

a wollastonite content of 30 wt%. After adding 40 wt% of wollastonite, T_{sinter} decreases again and with the addition of 50 wt% wollastonite the decrease is even higher. This means that the sintering of the last two samples is poor. Sintering stops before maximum densification has been reached. For this reason, the samples with 40 and 50 wt% of wollastonite were not further analyzed. The viscosity at the sintering temperature has to be decreased then around two orders of magnitude from 0 to 30% wollastonite containing samples in order to optimize the final density.

The crystalline phases of the sintered samples with 0, 10, 20, 30 wt% wollastonite are summarized in Table 4. As there was only a small amount of sample for each analysis, only the main crystalline phases could be identified.

A comparison of the XRD results for the samples with wollastonite contents of 0, 20 and 40 wt% can be found in Fig. 5. It can clearly be seen that the amount of crystalline phase from the aggregate (pseudowollastonite) increases with increasing amount of filler while the amount of anorthite which originates from the glass decreases. It was not possible to perform a Rietveld analysis on the results, but the comparison of the peak heights showed that the ratio of wollastonite to anorthite increased from 0.4 in the sample without addition of wollastonite to 1.1 (20 wt% of wollastonite) and to 3.1 (40 wt% of wollastonite). The other crystalline phases showed only small peaks and for this reason their relative contents were not evaluated.

Table 4
Crystalline phases in the sintered samples by XRD.

Sample	Phases
0% wollastonite	Anorthite ($CaAl_2Si_2O_8$), wollastonite ($CaSiO_3$), pseudowollastonite ($CaSiO_3$)
10% wollastonite	Anorthite ($CaAl_2Si_2O_8$), wollastonite ($CaSiO_3$), pseudowollastonite ($CaSiO_3$)
20% wollastonite	Anorthite ($CaAl_2Si_2O_8$), wollastonite ($CaSiO_3$), pseudowollastonite ($CaSiO_3$)
30% wollastonite	Anorthite ($CaAl_2Si_2O_8$), wollastonite ($CaSiO_3$), pseudowollastonite

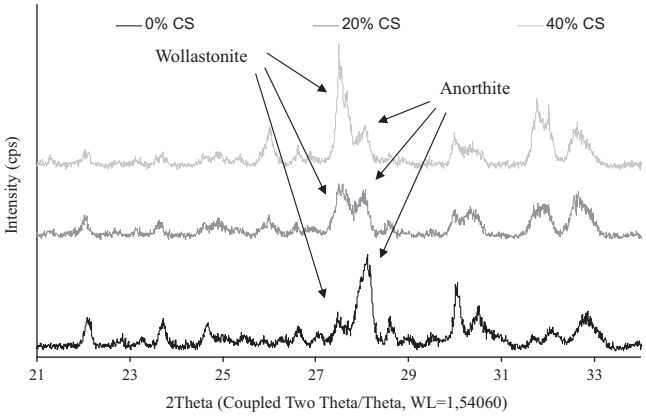

Fig. 5. Comparison of the XRD results of the different samples.

For characterizing the microstructure of the crystallized glass, SEM micrographs were taken. Porosity and occurrence of crystalline phases were evaluated (Figs. 6–9). The results of the porosite analysis can be seen in Table 5. The porosity increases a little with increasing amount of wollastonite, but is still low enough to ensure gas tightness also for the sample with 30 wt% wollastonite.

As can be seen from the figures, all samples show a certain amount of porosity. For the samples containing 0, 10, 20 and 30 wt% wollastonite the porosity is not percolating and the sintering of the samples is almost complete. The density of these samples is in the range of the density of the original powder (see Fig. 10) although this is not crystallized and therefore its density can only be regarded as a rough estimation of the density of the crystallized glass which will most probably show a different density than the original glass.

Crystallization can be observed in all samples. The crystallization did not lead to formation of pores or cracks which means that it has no influence on the gas tightness of

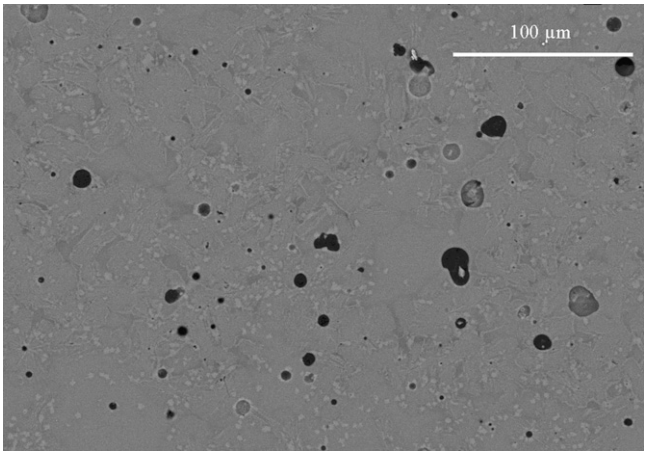

Fig. 6. SEM micrograph, sample without wollastonite, magnification 1000 × .

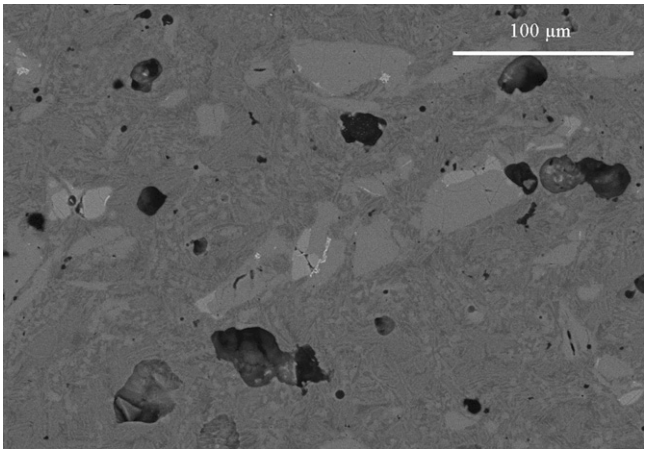

Fig. 7. SEM micrograph, sample with 10 wt% wollastonite, magnification 1000 × .

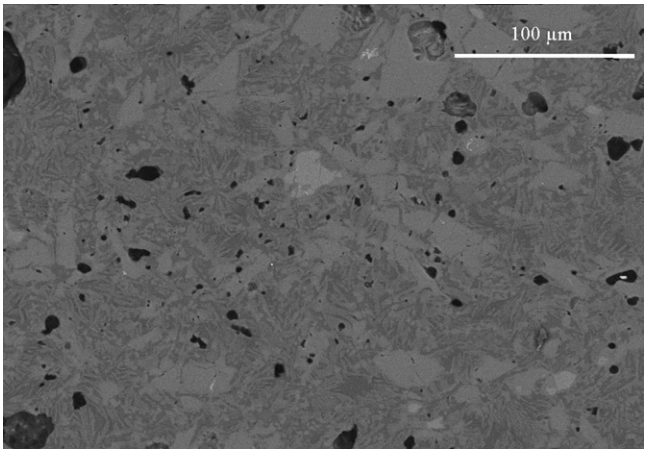

Fig. 8. SEM micrograph, sample with 20 wt% wollastonite, magnification 1000 × .

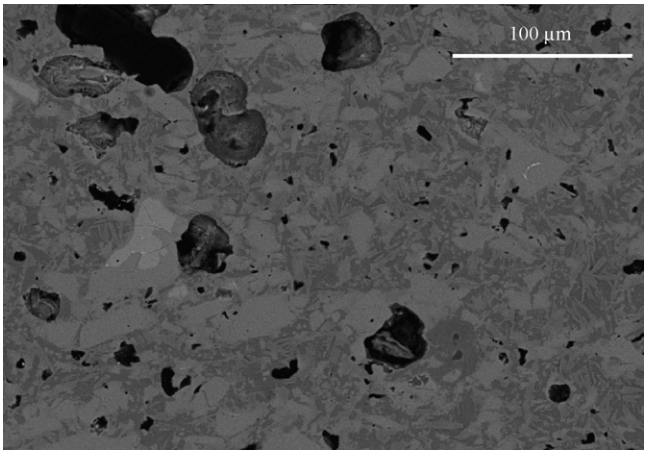

Fig. 9. SEM micrograph, sample with 30 wt% wollastonite, magnification 1000 × .

Table 5
Porosity of the samples determined from SEM pictures.

Sample	Porosity in %
0% wollastonite	2.0
10% wollastonite	4.3
20% wollastonite	4.6
30% wollastonite	7.0

the solder. With rising amount of wollastonite, the amount of crystals also increases showing that the wollastonite crystals act as a nucleating agent during the crystallization of the glass matrix.

The wollastonite grains in all the samples show sharp boundaries which shows that wollastonite is not dissolved in the glass. This was expected as wollastonite is one of the coexisting phases of the glass.

Due to their sufficiently high density and their small amount of non-percolating pores it can be said that the mixtures with 0, 10, 0 and 30 wt% wollastonite are

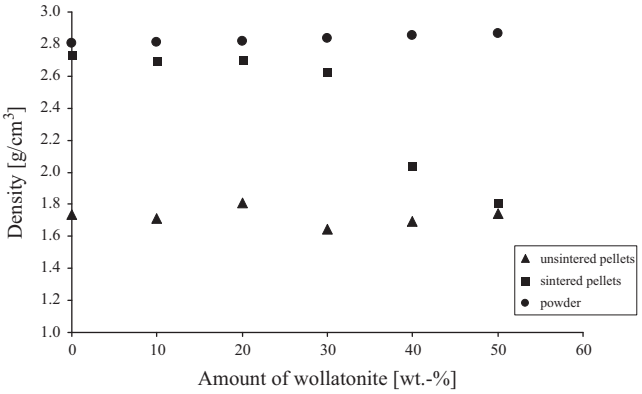

Fig. 10. Densities of the sintered pellets, the unsintered powders and the unsintered pellets.

applicable as solders for ceramic components. The other samples can most certainly not provide the required strength and gas tightness.

At the moment, the sealing properties for the sealing of Al_2O_3-ceramics are investigated together with the Forschungszentrum Juelich. These results will be published later.

4. Conclusions

A maximum amount of 30 wt% wollastonite can be added to the studied glass composition in order to obtain well densified composite materials with potential application as solders for ceramic components. The necessary increase of the sintering temperature in order to optimize the final density of the 30 wt% wollastonite-containing samples in comparison to the wollastonite-free material means a decrease of glass viscosity by two orders of magnitude.

The ratio of wollastonite to anorthite in the samples increases from 0.4 in the sample without wollastonite to 1.1 (20 wt% wollastonite) and 3.1 (40 wt% wollastonite) in terms of the corresponding intensities of the XRD peaks. Wollastonite grains are not dissolved in the glass as expected since wollastonite is one of the coexisting phases of the studied glass system.

Acknowledgements

This work was supported by the Integrated Action Spain-Germany DE2009-0069 and the DAAD (PPP Spanien, project-ID 50262236).

References

[1] T. Takami, Treatise on Materials Science and Technology, in: M. Tomozawa, R.H. Doremus (Eds.), Academic Press, New York, 17 (1979) pp. 173–255.
[2] N.N. Singhdeo, R.W. Schukle, Glass Science and Technology, Processing, in: D.R. Uhlman (Eds.), N.J. Kreidl, Academic Press, Orlando, (2) 1984, pp. 169–207.

[3] I.W. Donald, Preparation, properties and chemistry of glass and glass-ceramic-to-metal seals and coatings, Journal of Materials Science 28 (1993) 2841–2886.
[4] K.A. Nielsen, M. Solvang, S.B.L. Nielsen, A.R. Dinesen, D. Beeaff, P.H. Larsen, Glass composite seals for SOFC application, Journal of the European Ceramic Society 27 (2007) 1817–1822.
[5] S. Sakuragi, Y. Funahashi, T. Suzuki, Y. Fujishiro, M. Awano, Non-alkaline-MgO composites for SOFC sealant, Journal of Power Sources 185 (2008) 1311–1314.
[6] E. Wanko, Entwicklung eines neuen konzepts zur steuerung der thermischen ausdehnung von glaskeramischen verbundwerkstoffen mit angepasster fliessfähigkeit am beispiel der hochtemperaturbrennstoffzelle, Schriften des Forschungszentrums Jülich Reihe Energie & Umwelt/Energy & Environment 105 (2010).
[7] Fügen von keramischen Bauteilen durch laserinduziertes Löten – neue Simulationstools erschließen eine innovative Technologie, Verbundprojekt CeraJoin: Abschlussbericht Teil I und II, Förderkennzeichen BMBF 03 × 0507–030507–03 × 0507E, TIB/UB Hannover (2010).
[8] M.J. Pascual, A. Durán, M.O. Prado, A new method for determining fixed viscosity points of glasses, Physics and Chemistry of Glasses 46 (5) (2005) 512–520.